Low-Voltage Phase Shifters Based on $Hf_xZr_{1-x}O_2$ Ferroelectrics Integrated with Phased Antenna Arrays

M. Dragoman[#1], M. Aldrigo[#2], S. Iordanescu[#3], M. Modreanu[*4], I. Povey[*5], D. Vasilache[#6], A. Dinescu[#7], and C. Romanitan[#8]

[#]National Institute for Research and Development in Microtechnologies (IMT), Bucharest, Romania

[*]Tyndall National Institute, Cork, Ireland

{[1]mircea.dragoman, [2]martino.aldrigo, [3]sergiu.iordanescu, [6]dan.vasilache, [7]adrian.dinescu, [8]cosmin.romanitan}@imt.ro, {[4]mircea.modreanu, [5]ian.povey}@tyndall.ie

***Abstract* — In this paper, we present the design, fabrication and microwave experimental characterisation of a ferroelectric phase shifter, which is integrated with a 2-element antenna array to achieve beam-steering capabilities at very low voltages of ±1 V. The phase shifter consists of an interdigitated metallic capacitor deposited on a Zr-doped ferroelectric hafnium dioxide ($Hf_xZr_{1-x}O_2$) thin film, directly grown on high-resistivity Silicon (HR Si). The phase shifter shows a maximum phase shift of 53.74° at 2.55 GHz, sweeping the DC voltage between -1 V and +1 V. The miniaturised phased array is in the form of two gold patch antennas, phase shifters and additional circuitry, all integrated on $Hf_xZr_{1-x}O_2$/HR Si 4-inch wafer. The radiation beam at 2.55 GHz is steered with 25° when the 7-nm-thick ferroelectric is biased with ±1 V. These new microwave devices represent a step forward in the realisation of low-voltage tunable microwave components for the upcoming 5G technology.**

***Keywords* — Phased arrays, ferroelectric films, thin film devices.**

I. Introduction

Hafnium dioxide (HfO_2) is a well-known high-κ dielectric, widely used as gate insulator in transistors and microprocessors for very-large-scale integrated circuits. The ferroelectric phase in doped HfO_2 thin films (i.e. just few-nm thick) is related to an orthorhombic crystalline structure [1-3]. In what follows, Zr-doped HfO_2 is the chemical compound $Hf_xZr_{1-x}O_2$ (to which we will refer further as HfZrO), where $x = 0.45$ is the concentration of Hf, measured by XPS. We note that HfZrO ferroelectric materials exhibits other interesting properties, such as piezoelectric [4] and pyroelectric response [5].

Two important properties are envisaged by ferroelectrics based on doped HfO_2: (i) full CMOS compatibility; (ii) low energy consumption. The latter represent the main advantages of HfZrO with respect to perovskite ferroelectrics, widely used as microwave (MW) materials with tunable electric characteristics. For example, to obtain a significant phase shift in the MW band using perovskite ferroelectrics, tens of Volts are required, at the expense of relatively high losses [6]. The authors have already obtained very promising results in the domain of HfO_2-based ferroelectrics for MW applications, providing first a theoretical investigation [7] and then the experimental confirmation [8] of the great potentialities offered by few-nm-thick HfZrO for tunable phase shifters and other microwave devices in the 1–11 GHz frequency range.

One of the most important applications of phase shifters in the MW band is their integration in the so-called phased antenna arrays (PAAs) [9], having a radiation pattern that is the combination of the electromagnetic interference of the individual array elements through different excitation phases. In the view of the upcoming 5G wireless communication systems, specific bands (such as 2.3 GHz and 2.6 GHz) may be of particular interest, since they will be the key (as backbone) to implement the 5G broadband coverage: in detail, the mobile spectrum bands below 6 GHz will be of utmost importance to allow the smooth migration from LTE usage to 5G. In this respect, there is a great need of miniaturised phased antenna arrays with low-voltage beam-steering capabilities.

This paper presents a research carried out on HfZrO ferroelectric thin films for a practical application of PAAs at 2.55 GHz. The PAA consists of two gold patch antennas, each one connected to a phase shifter in order to bias the two antennas with different voltages, thus maximising the beam-steering effect.

In Section II, we provide first the electromagnetic (EM) design of both HfZrO-based phase shifter and PAA, with a brief description of the fabrication process; in Section III, we show the 3D full-wave simulations of the phase shifter, with a comparison with the relative full DC characterisation and MW measurements; finally, in Section IV an *in-depth* investigation of the performance of the HfZrO-based PAA is presented, with a discussion about the advantages of the proposed device and a particular emphasis on the scanning capabilities through the application of a low bias voltage. Some conclusions will be provided in Section V, together with future research in the domain of ferroelectric thin film components.

II. EM Design of the HfZrO-Based Phase Shifter and Phased Antenna Array

A. HfZrO-Based Phase Shifter

The HfZrO-based phase shifter consists of an interdigitated capacitor (IDC) in coplanar waveguide (CPW) technology. Fig. 1a shows the CST Microwave Studio® design (top-view) of the IDC/CPW structure (the inset is a magnification of the

IDC area), whereas Fig. 1b is an optical picture (top-view) of the fabricated device.

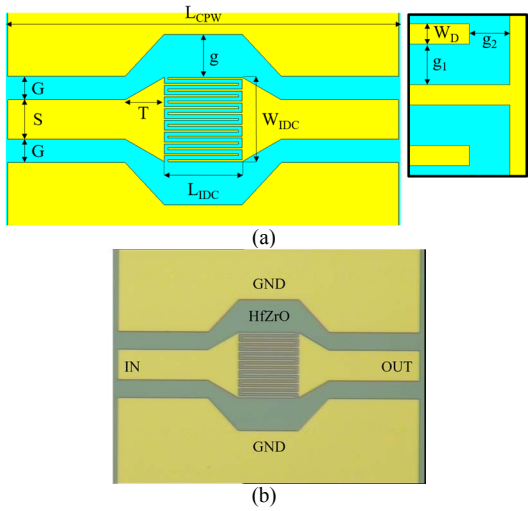

Fig. 1. (a) EM layout of the HfZrO-based IDC phase shifter with, in the inset, a detail of the digits; (b) optical picture of the fabricated device.

The HfZrO thin film was grown at 250 °C directly on a 525-µm-thick high-resistivity Silicon (HR Si, $\rho = 10000\ \Omega\cdot$cm, $\varepsilon_{HRSi} = 11.9$) 4-inch wafer by Atomic Layer Deposition (ALD). The film thickness value was confirmed by spectroscopic ellipsometry to be 7±0.2 nm using a four layer optical model: air/$Hf_xZr_{1-x}O_2$/SiO_2/HR Si. The composition of the HfZrO thin film was investigated by X-ray photoelectron spectroscopy (XPS): the ferroelectric film is clearly non-stoichiometric, exhibiting a significant oxygen deficiency. Then, the grazing incidence X-ray diffraction (GIXRD) pattern was measured, exhibiting two broad peaks, at around 30.5° and 55°, previously assigned to HfO_2 orthorhombic phase. Capacitance versus DC voltage and pulse-up negative-down (PUND) electrical tests were performed for electrical characterisation of the hysteretic nature of ferroelectric and its domain kinetics. We fabricated in the same batch vertical structures, i.e. capacitors made of Au/HfZrO/doped Si. Both electrical tests confirmed the typical behaviour of ferroelectricity in HfZrO, showing a coercive field $E_c = 1.2$ MV/cm and a remanent polarisation $P_r = 1.06\ \mu C/cm^2$ for as-grown metal-ferroelectric-semiconductor (MFS) capacitors and $P_r = 9.9\ \mu C/cm^2$ after electrical pulse poling, typical for HfZrO ferroelectrics [1, 2]. Finally, all the devices (i.e. phase shifters and the whole PAA) were fabricated via e-beam deposition of 500-nm-gold (Au) on the HfZrO/HR Si substrate. The IDC has 15 digits and, according to Fig. 1a, the main dimensions are the following: $L_{CPW} = 1$ mm $G = 60$ µm, $S = 100$ µm, $T = 100$ µm, $L_{IDC} = 200$ µm, $W_{IDC} = 215$ µm, $g = 110$ µm, $W_D = 5$ µm and $g_1 = g_2 = 10$ µm. The chosen G–S–G configuration guarantees the MW measurements by standard CPW 150-µm pitch probe tips. We found that the HfZrO thin film has a permittivity $\varepsilon_{HfZrO} = 30$–60 for an applied DC voltage $V_{DC} = \pm 3$ V [8]. This tunability of ε_{HfZrO} is the key factor in using HfZrO thin films: the IDC layout in CPW technology is beneficial from the technological point of view (since it is a planar structure that requires a single fabrication mask) and can be integrated very easily into a more complex circuit due to its compact dimensions. At the same time, the proposed IDC behaves as a variable capacitor (varactor) thanks to the presence of the underneath HfZrO layer: the application of the proper DC voltage entails a change in ε_{HfZrO}, which translates into a change of the capacitance C_{IDC} and allows tuning the phase constant $\beta_{IDC} = \omega\sqrt{(L_{IDC}\cdot C_{IDC})}$. The latter is responsible for the phase shift occurring in the MW signal passing through the IDC, assuming that L_{IDC} is constant.

B. *HfZrO-Based Phased Antenna Array*

In Fig. 2, we present the EM layout and fabrication of the proposed PAA.

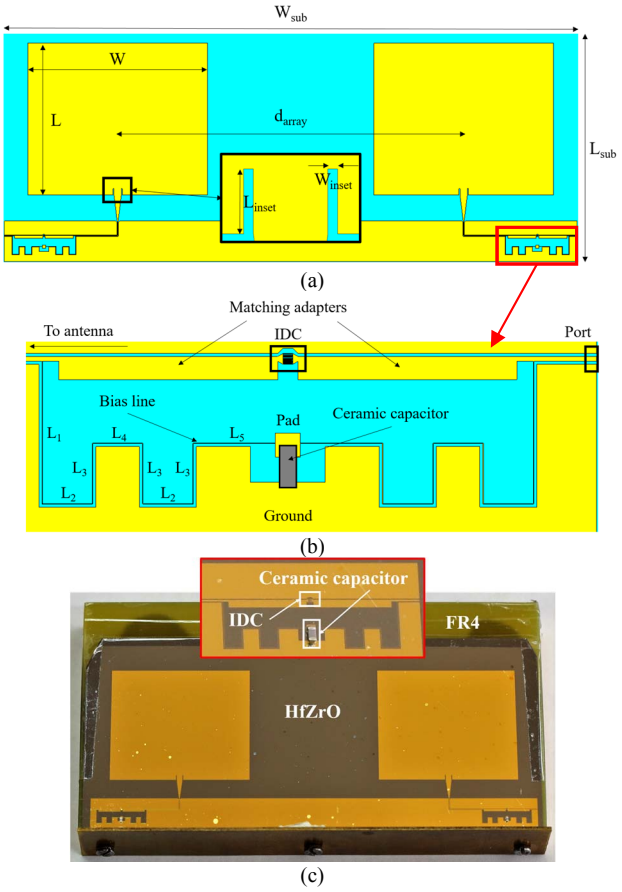

Fig. 2. (a) EM layout of the HfZrO-based PAA with a detail of the antenna inset; (b) detailed EM layout of the biasing network; (c) optical picture of the fabricated PAA with, in the inset, a detail of the biasing network.

In Fig. 2a, the CST Microwave Studio design of the HfZrO-based PAA is depicted. In this case, the main dimensions are: $W_{sub} = 89.4$ mm, $L_{sub} = 33.94$ mm, $W = 28$ mm, $L = 23.63$ mm, $d_{array} = 54$ mm $= 0.45\lambda_0$ ($\lambda_0 = 120$ mm is the free-space wavelength, whereas $\lambda_g \approx 45.28$ mm is the guided wavelength) for broadside radiation, $W_{inset} = 150$ µm and $L_{inset} = 1$ mm. Since the bias of each phase shifter is realised by applying the same polarity on both branches of the IDC (Fig. 1a), a smart *ad-hoc* biasing network was designed and simulated. In detail, a 12-µm-wide and $\lambda_g/4$-long line (in Fig. 2b, the thin line whose length is $L_1+2L_2+3L_3+L_4+L_5$) connects each port to a 500-µm-wide pad used to solder (with conductive paste) a 0402-type

ceramic capacitor of 4.7 pF; the capacitor resonates at the operating frequency, providing a short-circuit to the ground for both λ_g/4-lines, thus isolating the DC bias from the RF signal. In larger PAAs, for which multiple polarisations are needed, the bias can be applied through wires soldered on the pads (Fig. 2b) where the capacitors are assembled. A picture of the fabricated PAA is shown in Fig. 2c (in the inset, a detail of the biasing network). The PAA was designed to work around 2.5 GHz, hence in order to avoid any deterioration of matching and radiation characteristics due to the low thickness of the HR Si layer, the array was attached to a 3.2-mm-thick FR4 substrate to ensure a distance from the underneath metal plate (acting as a reflector) of at least λ_g/12 (instead of λ_g/86 with just the HR Si layer). This way, the broadside radiation performance of the PAA is guaranteed in the desired band. The thicker substrate also improves impedance matching, bandwidth and radiation efficiency.

In Fig. 1a and in Figs. 2a-b, the yellow colour is attributed to gold and the blue one to the underneath HfZrO layer.

III. EM Simulations and DC/Microwave Characterisation of HfZrO-Based Phase Shifter

A direct proof of the ferroelectricity in microwaves of the HfZrO thin films can be obtained by measurements in the 1–11 GHz range using an Anritsu 37397D Vector Network Analyser (VNA) connected to a SUSS PM5 probing station for electrical (DC and HF) measurements on wafers, with SOLT calibration standard. The setup is schematically represented in Fig. 3.

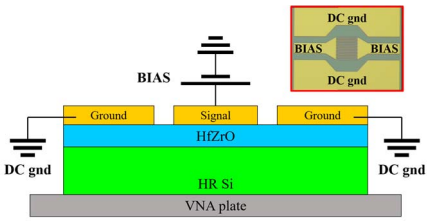

Fig. 3. Schematic representation of the DC/MW measurement setup (in the inset, an optical picture with the top-view of the HfZrO-based IDC is shown).

The IDC structures were biased by an external DC source, in order to control very precisely the supplied DC voltage. The bias is applied horizontally, thus conferring to the HfZrO thin film a DC polarisation via a horizontal electric field. The bias has the same polarity on both sides of the IDC, according to Fig. 3: this is the simplest way to bias independently each phase shifter of the PAA. Fig. 4a is a cross-section of the electrostatic 3D simulation of the IDC, whereas Fig. 4b is the comparison between 3D-simulated and measured transmission phase (i.e. phase of S_{21} – arg{S_{21}}) in the 1–11 GHz band at V_{DC} = 0 V. The maximum value of the static electric field (in correspondence of the gap between the digits and the lateral ground planes) is about 46 kV/m; furthermore, it is evident how the field is concentrated in the ferroelectric layer and decreases progressively in the HR Si substrate. The overall behaviour of the simulated arg{S_{21}} (or phase ϕ) is in rather good agreement with the measurements (also taking into account the very high aspect ratio – about 87500 – between the HfZrO thin film and the bulk HR Si, which could responsible for the differences between simulated and measured results).

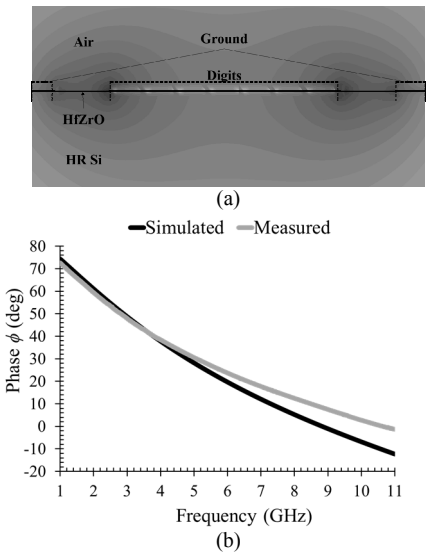

Fig. 4. (a) Cross-section of the IDC structure with the simulated distribution of the static electric field; (b) EM simulated (solid black line) and measured (solid grey line) arg{S_{21}} in the 1–11 GHz band at 0 V.

Finally, Fig. 5 displays the measured values of arg{S_{21}} (left vertical axis) and of the IDC capacitance C_{IDC} (right vertical axis) at 2.55 GHz as a function of the bias voltage V_{DC}.

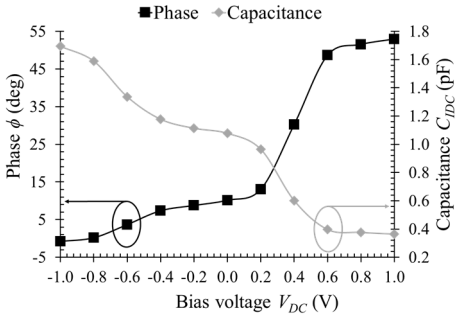

Fig. 5. Measured phase ϕ (left vertical axis, black line) and extracted IDC capacitance C_{IDC} (right vertical axis, grey line) of the HfZrO-based phase shifter at 2.55 GHz, as a function of the applied bias voltage V_{DC}.

The maximum phase shift $\Delta\phi = \phi_{+1} - \phi_{-1}$ is 53.76° when sweeping the DC voltage between -1 V and +1 V, whereas C_{IDC} varies in the range 0.36–1.69 pF. In the next future, we will try to extend the phase shift value up to at least 90° (or more) by considering novel material compositions and phase shifter layouts. The MW losses, in terms of insertion loss (IL), decrease with frequency and, in particular, at 0 V we have IL(0) = 6 dB at 2.55 GHz (becoming even 4 dB in the X band). If we consider the figure of merit FOM$_{°/dB}$ defined as FOM$_{°/dB}$ = $\Delta\phi$/IL(0), we obtain FOM$_{°/dB}$ = 9 °/dB at 2.55 GHz. However, if ΔV = 2 V is the DC voltage range necessary to obtain the above mentioned value for $\Delta\phi$, then we have FOM$_{°/\Delta V}$ = $\Delta\phi/\Delta V$ = 26.88 °/V at 2.55 GHz, whereas in [10] a BST-based phase shifter with FOM$_{°/dB}$ = 29 °/dB was obtained, but with FOM$_{°/\Delta V}$ = 0.277 °/V at 10 GHz, hence two orders of magnitude lower (even if at a different working frequency).

IV. EM Simulations and Microwave Characterisation of the HfZrO-Based Phased Antenna Array

In Fig. 6, the complete microwave experimental characterisation of the HfZrO-based PAA is provided.

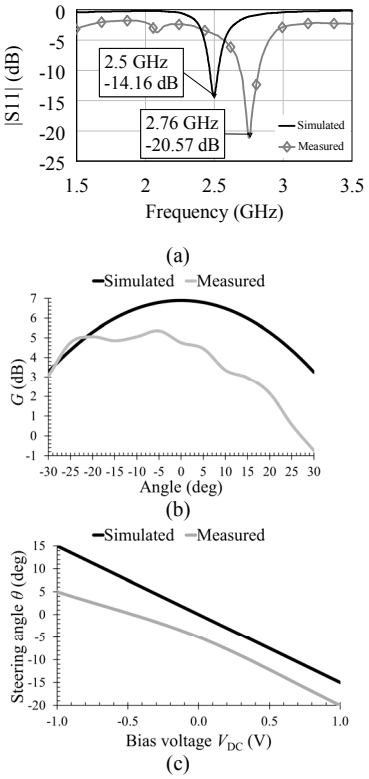

Fig. 6. (a) Simulated (solid black line) and measured (solid grey line with diamonds) $|S_{11}|$ of the single patch; (b) simulated (solid black line) and measured (solid grey line) G of the HfZrO-based PAA at 2.55 GHz for V_{DC} = 0 V; (c) simulated (solid black line) and measured (solid grey line) steering angle θ at 2.55 GHz as a function of the applied bias voltage V_{DC}.

Fig. 6a shows the simulated and measured return loss $|S_{11}|$ of the single patch antenna: the simulated value has a minimum at 2.5 GHz, whereas the measured value $|S_{11}|$ = -20.57 dB is at 2.76 GHz. The discrepancy (around 9%) could be due to: (i) the intrinsic difficulty of simulating the multi-layer structure made of HR Si and ferroelectric thin film; (ii) fabrication and FR4 permittivity tolerances. Nevertheless, the two patches in array configuration give a maximum of radiation at 2.55 GHz, as we verified by measuring the gain in a wide frequency range around 2.5 GHz. We performed measurements of the far-field/gain using as receiver a 16-dBi-gain reference antenna placed on a rotating arm, at various rotation angles in the range between -30° and +30°, with steps of 5°, and connected to an Anritsu MS2668C spectrum analyser. The HfZrO-based PAA was placed at 1.2-m distance from the reference antenna (about $10\lambda_0$, hence in the Fraunhofer region of the PAA) and connected to an Agilent E8257D PSG Analog Signal Generator through a 3-dB splitter and two bias tees used to bias separately the two patches. The angular range of ±30° was chosen to avoid excessive reflections from the table and other facilities surrounding the setup; nevertheless, the setup was not tested in an anechoic chamber and just one radiation plane was measured at the time of this work. In a first step, the far-field/gain of the HfZrO-based PAA were measured without applying any bias. The results for the gain G at 2.55 GHz for V_{DC} = 0 V are depicted in Fig. 6b. The measured direction of maximum gain (G_{max}) shows a small tilt (of 5°) due to a slight asymmetry in the power radiated by the two patches (due to different IL values of the phase shifters). The measured G_{max} is 5.36 dB, whereas the simulated value is 6.79 dB. The difference of 1.43 dB is due to different IL actual values of the phase shifters placed between each port and the corresponding patch antenna w.r.t. the standalone phase shifters with biasing networks (Fig. 2b): these differences could not be taken into account in the calculations for measured antenna gain, thus creating a numerical uncertainty. Finally, the simulated and measured steering angle θ of G_{max} (at 2.55 GHz) depending on V_{DC} is depicted in Fig. 6c. We see that applying a V_{DC} in the small range ±1 V allows steering the beam at 2.55 GHz with 25° totally, whereas the simulated angle range is 30°.

V. Conclusion

In this paper, we have demonstrated the proof-of-concept of a ferroelectric-based phased antenna array, able to steer the radiation pattern with 25° at 2.55 GHz for very low bias voltages of ±1 V, the array being low-profile and compact, hence suitable for next generation 5G low-power wireless applications. Future research will be focused on the design, fabrication and test of enhanced ferroelectric-based PAAs with increased steering angle.

References

[1] T. S. Böscke, J. Müller, D. Bräuhaus, U. Schröder, and U. Böttger, "Ferroelectricity in hafnium oxide thin films," *Appl. Phys. Lett.*, vol. 99, p. 102903, 2011.

[2] J. Müller, T. S. Böscke, U. Schröder, S. Mueller, D. Bräuhaus, U. Böttger, L. Frey, and T. Mikolajick, "Ferroelectricity in simple binary ZrO_2 and HfO_2," *Nano Lett.*, vol. 12, pp. 4318−4323, 2012.

[3] U. Schröder, S. Mueller, J. Mueller, E. Yarchuk, D. Martin, C. Adelmann, T. Schloesser, R. van Bentum, and T. Mikolajick, "Hafnium oxide based CMOS compatible ferroelectric materials," *ECS J. Solid State Science and Technology*, vol. 2, N69-N72, 2013.

[4] S. Starschich, T. Schenk, U. Schröder, and U. Böttger, "Ferroelectric and piezoelectric properties of $Hf_{1-x}Zr_xO_2$ and pure ZrO_2 films," *Appl. Phys. Lett.*, vol. 110, p. 182905, 2017.

[5] S. W. Smith, A. R. Kitahara, M. A. Rodriguez, M. D. Henry, M. T. Brumbach, and J. I. Ihlefeld, "Pyroelectric response in crystalline zirconium oxide ($Hf_{1-x}Zr_xO_2$) thin films," *Appl. Phys. Lett.*, vol. 110, p. 072901, 2017.

[6] A. Ahmed, I. A. Goldhorpe, and A. K. Khandani, "Electrically tunable materials for microwave applications," *Appl. Phys. Rev.*, vol. 2, p. 011302, 2015.

[7] M. Dragoman, M. Aldrigo, M. Modreanu, and D. Dragoman, "Extraordinary tunability of high frequency devices using $Hf_{0.3}Zr_{0.7}O_2$ ferroelectric at very low applied voltages," *Appl. Phys. Lett.*, vol. 110, p. 103104, 2017.

[8] M. Dragoman, M. Modreanu, I. M. Povey, S. Iordanescu, M. Aldrigo, C. Romanitan, D. Vasilache, A. Dinescu, and D. Dragoman, "Very large phase shift of microwave signals in a 6nm $Hf_xZr_{1-x}O_2$ ferroelectric at ±3 V," *Nanotechnology*, vol. 28, 38LT04, 2017.

[9] R. C. Hansen, *Phased Array Antennas*, 2nd ed., John Wiley and Sons, New York, 2009.

[10] M. Haghzadeh, C. Armiento, and A. Akyurtlu, "All-Printed Flexible Microwave Varactors and Phase Shifters Based on a Tunable BST/Polymer," *IEEE Trans. on Microwave Theory and Tech.*, vol. 65, no. 9, pp. 2030–2042, Jun. 2017.